Journal of Computational Physics 335 (2017) 905–924

Contents lists available at ScienceDirect

Journal of Computational Physics

www.elsevier.com/locate/jcp

# A stochastic asymptotic-preserving scheme for a kinetic-fluid model for disperse two-phase flows with uncertainty

Shi Jin [a,b,*,1], Ruiwen Shu [a]

[a] Department of Mathematics, University of Wisconsin–Madison, Madison, WI 53706, USA
[b] Institute of Natural Sciences, School of Mathematical Science, MOELSEC and SHL-MAC, Shanghai Jiao Tong University, Shanghai 200240, China

ARTICLE INFO

*Article history:*
Received 2 October 2016
Received in revised form 24 January 2017
Accepted 25 January 2017
Available online 1 February 2017

*Keywords:*
Kinetic-fluid model
Disperse particles
Uncertain quantification
Asymptotic-preserving
Projection method
Stochastic Galerkin

ABSTRACT

In this paper we consider a kinetic-fluid model for disperse two-phase flows with uncertainty. We propose a stochastic asymptotic-preserving (s-AP) scheme in the generalized polynomial chaos stochastic Galerkin (gPC-sG) framework, which allows the efficient computation of the problem in both kinetic and hydrodynamic regimes. The s-AP property is proved by deriving the equilibrium of the gPC version of the Fokker–Planck operator. The coefficient matrices that arise in a Helmholtz equation and a Poisson equation, essential ingredients of the algorithms, are proved to be positive definite under reasonable and mild assumptions. The computation of the gPC version of a translation operator that arises in the inversion of the Fokker–Planck operator is accelerated by a spectrally accurate splitting method. Numerical examples illustrate the s-AP property and the efficiency of the gPC-sG method in various asymptotic regimes.



## 1. Introduction

In this paper, we are concerned with kinetic-fluid models for disperse two-phase flows. Such models arise naturally in the study of mixture of a continuum of fluid, such as gas and liquids, and small particles, such as droplets and suspension of solids. The fluid phase is described by hydrodynamic equations, such as the Euler equations or the Navier–Stokes equations, while the particle phase is described by a kinetic equation. The application of kinetic-fluid models includes the dynamic of sprays [7,25,17], granular flows [1,9,6], and combustion theory [10,26], to name a few.

We focus on the model where the fluid phase has small compressibility and nonzero viscosity, thus modeled by the incompressible Navier–Stokes (NS) equations. The particles are assumed to be subjected to a drag force obeying the Stokes Law, i.e., proportional to the relative velocity of the particle and the fluid. Furthermore, the particles are subject to an external force field (gravity, for example) and Brownian motions. For simplicity we take the physical space to be 2-dimensional. The model is given by

* Corresponding author.
*E-mail addresses:* sjin@wisc.edu (S. Jin), rshu2@math.wisc.edu (R. Shu).

[1] This author's research was supported by NSF grants DMS-1522184 and DMS-1107291: RNMS KI-Net, by NSFC grant No. 91330203, and by the Office of the Vice Chancellor for Research and Graduate Education at the University of Wisconsin–Madison with funding from the Wisconsin Alumni Research Foundation.

http://dx.doi.org/10.1016/j.jcp.2017.01.059
0021-9991/

$$\begin{cases} \partial_t f + v\cdot\nabla_x f - \nabla_x\Phi\cdot\nabla_v f = \dfrac{1}{\epsilon}\mathcal{L}_u f, \\ \partial_t u + \nabla_x\cdot(u\otimes u) + \nabla_x p - \dfrac{1}{Re}\Delta_x u = \dfrac{1}{\epsilon}\kappa\displaystyle\int (v-u) f\,\mathrm{d}v, \\ \nabla_x\cdot u = 0, \end{cases} \tag{1.1}$$

where $\mathcal{L}_u f$ is the Fokker–Planck (FP) operator

$$\mathcal{L}_u f = \nabla_v\cdot((v-u)f + \nabla_v f). \tag{1.2}$$

$x = (x_1, x_2) \in \Omega \subset \mathbb{R}^2$ is the space variable, and $v = (v_1, v_2) \in \mathbb{R}^2$ is the velocity variable. $f = f(t, x, v)$ is the density function of the particles. $u = u(t, x) = (u^{(1)}(t, x), u^{(2)}(t, x))$ is the velocity field of the fluid. $\Phi = \Phi(x)$ is an external force field. The first equation describes the motion of particles. The two terms in the FP operator comes from the drag force from the fluid and the effect of Brownian motions, respectively. The $\nabla_x\Phi$ term is the effect of the external force field on the particles. The second and third equations are the standard Navier–Stokes equations for the fluid, with the right-hand-side term describing the force coming from the particle. $\kappa > 0$ is the coupling constant depending on the strength of interaction between the particles and the fluid, and $Re$ is the Reynolds number. $\epsilon$ is the Knudsen number given by $\epsilon = \frac{2\rho_P a^2}{9\mu}$, where $\mu$ is the dynamic viscosity of the fluid, $a$ the typical radius of the particles, and $\rho_P$ the density of the particles.

The hydrodynamic limit of this model was first investigated by Goudon et al. [11,12] in two different regimes. We follow the scaling given in [12], which is called the fine particle regime.

In [13] Goudon et al. proposed an Asymptotic-Preserving (AP) [18] scheme for the two-phase flow system (1.1), which are efficient for both the cases of small and large $\epsilon$. The main idea of this work is to incorporate the evolution of the moments of the particles into the projection method [5,27] for the NS system. The possibly stiff (when $\epsilon$ is small) FP operator is treated fully implicitly, with a well-balanced spatial discretization proposed by Jin and Yan [19]. The second order time discretization is given by the backward difference.

The paper [13] only concerns with the case where all the physical quantities and parameters are deterministic. However, there are many sources of uncertainties in this model. For example, the initial data of $f$ and $u$ come from experimental measurements, hence may have measurement errors. If one adopts the Maxwellian boundary condition for $f$ with the accommodation coefficient, or the no-slip boundary condition for $u$ against a wall with a nonzero velocity, then these boundary data will contain parameters, which come from direct measurements or matching with experimental data. Such parameters will also give rise to uncertainties. Furthermore, the parameters $\epsilon, \kappa, Re$ and the external field $\Phi$ come from measurements and have uncertainties. To provide reliable predictions and a guidance to improve the model, it is imperative to incorporate these uncertainties into the system, and quantify these uncertainties by numerically solving the resulting system with uncertain inputs.

In the last two decades, a large variety of numerical methods have been developed in the field of uncertainty quantification (UQ) [8,16,22,28,29]. Among these methods, the most popular ones are Monte-Carlo methods [23], stochastic collocation methods [2,4,24,30] and stochastic Galerkin methods [4,3]. The idea of Monte-Carlo methods is to sample randomly in the random space, which results in halfth order convergence. Stochastic collocation methods use sample points on a well-designed grid, and one can evaluate the statistical moments by numerical quadratures. Stochastic Galerkin methods start from an orthonormal basis in the random space, and approximate functions by truncated polynomial chaos expansions. By the Galerkin projection, a deterministic system of the expansion coefficients can be obtained. While Monte-Carlo methods have advantage in very high dimensional random spaces, the other two methods can achieve spectral accuracy if one adopts the generalized polynomial chaos (gPC) basis [31], which is a great advantage if the dimension of the random space is not too high. In this paper we focus on low dimensional random spaces, and adopt the stochastic Galerkin approach.

To effectively handle possible multiscales, where $\epsilon$ can be small or large, the AP approach has been proved to be very effective for (deterministic) kinetic problems (see [18,20]). For kinetic problems with uncertainties, the gPC based stochastic Galerkin (gPC-sG) method introduces a deterministic system which is basically a vector version of the deterministic counterparts, thus allowing one to utilize the deterministic AP framework to handle uncertain problems, in the sense of stochastic Asymptotic-Preserving (s-AP) [21]. A scheme is s-AP if the stochastic Galerkin (sG) method for the uncertain kinetic equation approaches to the sG method of the limiting (macroscopic) hydrodynamic equations as $\epsilon \to 0$. In this paper we adopt this approach, and propose an s-AP scheme for the kinetic-fluid model with uncertainties. In order to simplify the presentation and emphasize the main idea, we only consider the case of uncertain initial data. Uncertainties from other terms can be treated similarly in the sG framework, see [33].

Compared with the deterministic problem in [13], there are several new difficulties to overcome. First, the formal proof of the s-AP property is less obvious, due to the vector form of the scheme. Our proof is based on the observation that the gPC version of the FP operator $\vec{\mathcal{L}}$ is the deterministic FP operator $\mathcal{L}_0$ conjugated by a gPC version of the translation operator $\vec{\mathcal{T}}$ (see Section 3.3 for details). This observation gives rise to the equilibrium of $\vec{\mathcal{L}}$, and thus the hydrodynamic limit of the gPC system follows as $\epsilon \to 0$, which allows us to justify the s-AP property. Second, one needs to show that the resulted Helmholtz and Poisson systems, essential ingredients of the s-AP schemes, are well-defined systems. Indeed these properties, which are based on the positive-definiteness of the coefficient matrices in these systems, will be proven under reasonable and mild assumptions. Thirdly, to treat $\vec{\mathcal{L}}$ implicitly, which is needed for good numerical stability property, it is

necessary to compute the translation operator $\vec{\mathcal{T}}$, which is very expensive if computed directly. We accelerate this computation dramatically by using a spectrally accurate splitting together with the Fast Fourier Transform. Then the problem is reduced to the inversion of $\mathcal{L}_0$, which can be easily and efficiently computed by the method for the deterministic Fokker–Planck system in [19]. As a result, we just need to diagonalize *two* matrices of size $K+1$ in each time step, while the direct method needs to diagonalize $N_v^2$ such matrices, where $K$ is the degree of orthogonal polynomials and $N_v$ the number of mesh points in the one-dimensional velocity space.

The paper is organized as follows: in Section 2 we briefly review the hydrodynamic limit of the deterministic problem; in Section 3 we propose the gPC approximation to the problem with uncertain initial data, and prove the s-AP property of the gPC-sG method; in Section 4 we give the fully discrete s-AP scheme, prove the positive-definiteness of two coefficient matrices, and give a spectrally accurate splitting method for the translation operator $\vec{\mathcal{T}}$; in Section 5 we demonstrate the s-AP property and the efficiency of the gPC-sG method by some numerical examples. The paper is concluded in Section 6.

## 2. The deterministic problem

In this section we briefly review the results for the deterministic problem. The hydrodynamic limit of the system (1.1) was proved in [11,12]. Here we give a formal derivation of the limit.

Define the moments

$$n(t,x)=\int f(t,x,v)\,\mathrm{d}v,\quad J(t,x)=\int vf(t,x,v)\,\mathrm{d}v,\quad P(t,x)=\int v\otimes vf(t,x,v)\,\mathrm{d}v. \tag{2.1}$$

Define the local Maxwellian as

$$M_u(v)=\frac{1}{2\pi}\exp(-\frac{|v-u(t,x)|^2}{2}). \tag{2.2}$$

First note that

$$\mathcal{L}_u f=\nabla_v\cdot\left(M_u\nabla_v\left(\frac{f}{M_u}\right)\right), \tag{2.3}$$

which implies that $\mathcal{L}_u$ is a self-adjoint operator on $L^2_u(\mathbb{R}^2)$, defined as the weighted $L^2$ space with weight $M_u^{-1}$. Denote the inner product on $L^2_u(\mathbb{R}^2)$ by $\langle f,g\rangle=\int fgM_0^{-1}\,\mathrm{d}v$. Then one has the coercivity estimate

$$\langle f,\mathcal{L}_u f\rangle=-\int M_u\left|\nabla_v\left(\frac{f}{M_u}\right)\right|^2\,\mathrm{d}v\le 0, \tag{2.4}$$

which implies that the null space of $\mathcal{L}_u$ is one dimensional, spanned by $M_u$.

As $\epsilon\to 0$ in (1.1), one formally has $\mathcal{L}_u f=0$, which implies

$$f(t,x,v)=n(t,x)M_u(v). \tag{2.5}$$

This implies

$$J=nu,\quad P=nu\otimes u+nI, \tag{2.6}$$

where $I$ is the identity matrix. Integrating the first equation of (1.1) in $v$ against $1, v$, one has

$$\partial_t n+\nabla_x\cdot J=0, \tag{2.7}$$

$$\partial_t J+\nabla_x\cdot P=-\frac{1}{\epsilon}\int(v-u)f\,\mathrm{d}v+n\nabla_x\Phi. \tag{2.8}$$

Then multiplying (2.8) by $\kappa$ and adding it to the second equation of (1.1), using (2.6), one gets

$$\begin{cases}\partial_t n+\nabla_x\cdot(nu)=0,\\ \partial_t((1+\kappa n)u)+\nabla_x((1+\kappa n)u\otimes u)+\nabla_x(p+\kappa n)+\kappa n\nabla_x\Phi=\dfrac{1}{Re}\Delta_x u,\end{cases} \tag{2.9}$$

which is the incompressible Navier–Stokes equations with variable density $(1+\kappa n)$.

## 3. The gPC approximation to the problem with uncertainty

We consider the same system with $f$ and $u$ depending on an extra random variable $z$:

$$\begin{cases} \partial_t f + \nabla_x f - \nabla_x \Phi \cdot \nabla_v f = \dfrac{1}{\epsilon}\mathcal{L}_u f, \\ \partial_t u + \nabla_x \cdot (u \otimes u) + \nabla_x p - \dfrac{1}{Re}\Delta_x u = \dfrac{1}{\epsilon}\kappa \displaystyle\int (v-u) f \, \mathrm{d}v, \\ \nabla_x \cdot u = 0, \end{cases} \tag{3.1}$$

where $f = f(t, x, v, z)$, $u = u(t, x, z)$. The random variable $z$ with a probability distribution $\pi(z)\,\mathrm{d}z$, describes the uncertainties in the model. In reality, such uncertainty often comes from initial data, boundary data and parameters in the model ($\kappa$, $Re$). For clarity of the presentation, we only consider the uncertainty from initial data. Uncertainties from other sources can be similarly treated under the same framework, see [33].

### 3.1. The generalized polynomial chaos (gPC) expansion

Denote $\{\phi_j(z)\}_{j=0}^{\infty}$ to be the gPC basis with respect to $\pi(z)$, which means that $\phi_j(z)$ is a polynomial of degree $j$, and these polynomials form an orthonormal basis of $L^2(\pi(z)\,\mathrm{d}z)$. Denote

$$f_j = \int f(z)\phi_j(z)\,\mathrm{d}z, \tag{3.2}$$

to be the $j$-th gPC coefficient of a function $f(z)$. Then $f$ can be approximated by a truncated gPC series

$$f(z) = \sum_{j=0}^{\infty} f_j \phi_j(z) \approx \sum_{j=0}^{K} f_j \phi_j(z) := f^K(z). \tag{3.3}$$

When $f$ is smooth, this approximation has spectral accuracy, i.e.,

$$\| f - f^K \|_{L_z^2} \le \frac{C_m}{K^m} \| f \|_{H_z^{m+1}}, \quad \forall m \ge 1. \tag{3.4}$$

The gPC coefficients of the product of two functions $f(z)$ and $g(z)$ can be approximated by using the following expression

$$(fg)_k = \sum_{i,j=0}^{\infty} S_{ijk} f_i g_j \approx \sum_{i,j=0}^{K} S_{ijk} f_i g_j, \tag{3.5}$$

where $S_{ijk}$ is given by

$$S_{ijk} = \int \phi_i(z)\phi_j(z)\phi_k(z)\pi(z)\,\mathrm{d}z. \tag{3.6}$$

This is called the spectral convolution. The gPC coefficients of the quotient of two functions $f(z)$ and $g(z)$ can be approximated from the relation

$$(f)_k = \sum_{i,j=0}^{\infty} S_{ijk} (f/g)_i g_j \approx \sum_{i,j=0}^{K} S_{ijk} (f/g)_i g_j. \tag{3.7}$$

This is a linear equation for $\{(f/g)_i\}_{i=0}^{K}$. The coefficient matrix

$$A_{ik} = \sum_{j=0}^{K} S_{ijk} g_j \tag{3.8}$$

is symmetric, and positive definite if $g^K(z)$ is positive everywhere. This can be seen by

$$\sum_{i,k=0}^{K} A_{ik}\xi_i\xi_k = \int g^K(z) \left( \sum_{i=0}^{K} \xi_i \phi(z) \right)^2 \pi(z)\,\mathrm{d}z > 0, \quad \forall \vec{\xi} \ne 0. \tag{3.9}$$

Thus in such case $\{(f/g)_i\}_{i=0}^{K}$ is always solvable, and can be solved by any numerical linear equation solver for positive definite matrices, for example, the conjugate gradient method.

### 3.2. Equations for the gPC coefficients

We use a stochastic Galerkin method based on the gPC expansions. We approximate the quantities $f$ and $u$ by a truncated gPC expansion:

$$f(t,x,v,z)=\sum_{k=0}^{\infty} f_k(t,x,v)\phi_k(z)\approx\sum_{k=0}^{K} f_k(t,x,v)\phi_k(z):=f^K(t,x,v,z), \tag{3.10}$$

$$u(t,x,z)=\sum_{k=0}^{\infty} u_k(t,x)\phi_k(z)\approx\sum_{k=0}^{K} u_k(t,x)\phi_k(z):=u^K(t,x,z). \tag{3.11}$$

Substituting these approximations into (3.1), multiplying by $\phi_j(z)$ and integrating with respect to $\pi(z)\,\mathrm{d}z$, one gets

$$\begin{cases}\partial_t f_j+v\cdot\nabla_x f_j-\nabla_x\Phi\cdot\nabla_v f_j=\dfrac{1}{\epsilon}(\mathcal{L}_u f^K)_j,\\ \partial_t u_j+\nabla_x\cdot(u^K\otimes u^K)_j+\nabla_x p_j-\dfrac{1}{Re}\Delta_x u_j=\dfrac{1}{\epsilon}\kappa\displaystyle\int((v-u^K)f^K)_j\,\mathrm{d}v,\\ \nabla_x\cdot u_j=0,\end{cases} \tag{3.12}$$

where the sub-index $j=0,\dots,K$. This is a deterministic system of the gPC coefficients $\{f_j\}_{j=0}^K$ and $\{u_j\}_{j=0}^K$.

With a chosen $K$, for a function $g=g(z)\approx g^K$, we introduce the notation

$$\begin{aligned}&\vec{g}=(g_0,\dots,g_K)^T,\\ &A(g)\text{ is a size }K+1\text{ matrix defined by }A(g)_{ij}=\sum_{k=0}^{K}S_{ijk}g_k.\end{aligned} \tag{3.13}$$

Then the system of gPC coefficients can be written as

$$\begin{cases}\partial_t\vec{f}+v\cdot\nabla_x\vec{f}-\nabla_x\Phi\cdot\nabla_v\vec{f}=\dfrac{1}{\epsilon}\vec{\mathcal{L}}_{\vec{u}}\vec{f},\\ \partial_t\vec{u}^{(i)}+\partial_{x_1}(A^{(i)}\vec{u}^{(1)})+\partial_{x_2}(A^{(i)}\vec{u}^{(2)})+\partial_{x_i}\vec{p}-\dfrac{1}{Re}\Delta_x\vec{u}^{(i)}=\dfrac{1}{\epsilon}\kappa\displaystyle\int(v_i-A^{(i)})\vec{f}\,\mathrm{d}v,\quad i=1,2,\\ \nabla_x\cdot\vec{u}=0,\end{cases} \tag{3.14}$$

where $\vec{\mathcal{L}}$ is the gPC version of the Fokker–Planck operator

$$\vec{\mathcal{L}}_{\vec{u}}(\vec{f})=\Delta_v\vec{f}+\partial_{v_1}(v_1\vec{f})+\partial_{v_2}(v_2\vec{f})-\partial_{v_1}(A^{(1)}\vec{f})-\partial_{v_2}(A^{(2)}\vec{f}), \tag{3.15}$$

and $A^{(1)},A^{(2)}$ are given by

$$A^{(1)}=A(u^{(1)}),\quad A^{(2)}=A(u^{(2)}), \tag{3.16}$$

and a term like $A^{(i)}\vec{u}^{(1)}$ or $A^{(i)}\vec{f}$ is interpreted as a matrix–vector multiplication.

### 3.3. The structure and coercivity of $\vec{\mathcal{L}}_{\vec{u}}$

We will analyze the structure of $\vec{\mathcal{L}}_{\vec{u}}$ and give a coercivity result as a generalization of (2.4). We begin with introducing the gPC version of the translation operator $\mathcal{T}_u$ on $L^2(\mathbb{R}^2,\mathbb{R}^{K+1})$ by

$$\vec{\mathcal{T}}_{\vec{u}}(\vec{f})=\exp(-A^{(1)}\partial_{v_1}-A^{(2)}\partial_{v_2})(\vec{f}). \tag{3.17}$$

In other words, $\vec{\mathcal{T}}_{\vec{u}}(\vec{f})$ is the solution at $s=1$ of the hyperbolic system

$$\partial_s\vec{g}(s,v)+A^{(1)}\partial_{v_1}\vec{g}+A^{(2)}\partial_{v_2}\vec{g}=0,\quad \vec{g}(0,\cdot)=\vec{f}(\cdot). \tag{3.18}$$

Note that this system is hyperbolic because $A^{(1)},A^{(2)}$ are symmetric. It is easy to see that $\vec{\mathcal{T}}_{\vec{u}}$ is a unitary operator, i.e., $\int\vec{\mathcal{T}}_{\vec{u}}\vec{f}\cdot\vec{\mathcal{T}}_{\vec{u}}\vec{g}\,\mathrm{d}v=\int\vec{f}\cdot\vec{g}\,\mathrm{d}v$. We first prove the following lemma:

**Lemma 3.1.**

$$\vec{\mathcal{T}}_{\vec{u}}[\partial_{v_1}(v_1\vec{f})+\partial_{v_2}(v_2\vec{f})]=\partial_{v_1}(v_1\vec{\mathcal{T}}_{\vec{u}}\vec{f})+\partial_{v_2}(v_2\vec{\mathcal{T}}_{\vec{u}}\vec{f})-(A^{(1)}\partial_{v_1}+A^{(2)}\partial_{v_2})\vec{\mathcal{T}}_{\vec{u}}\vec{f}. \tag{3.19}$$

**Proof.** Let $\vec{g}(s,v)$ be the solution of the hyperbolic system (3.18). Then

$$\begin{aligned}&\partial_s[\partial_{v_1}(v_1\vec{g})]\\ &=\partial_{v_1}[v_1(-A^{(1)}\partial_{v_1}-A^{(2)}\partial_{v_2})\vec{g}]\\ &=\partial_{v_1}[(-A^{(1)}\partial_{v_1}-A^{(2)}\partial_{v_2})(v_1\vec{g})+A^{(1)}\vec{g}]\\ &=(-A^{(1)}\partial_{v_1}-A^{(2)}\partial_{v_2})\partial_{v_1}(v_1\vec{g})+A^{(1)}\partial_{v_1}\vec{g}\end{aligned} \tag{3.20}$$

Writing a similar expression for the second component of $v$ and adding together, one gets

$$\begin{aligned}&\partial_s[\partial_{v_1}(v_1\vec{g})+\partial_{v_2}(v_2\vec{g})]\\ &=(-A^{(1)}\partial_{v_1}-A^{(2)}\partial_{v_2})[\partial_{v_1}(v_1\vec{g})+\partial_{v_2}(v_2\vec{g})]+(A^{(1)}\partial_{v_1}+A^{(2)}\partial_{v_2})\vec{g}\end{aligned} \tag{3.21}$$

Then

$$\begin{aligned}&\partial_s[\partial_{v_1}(v_1\vec{g})+\partial_{v_2}(v_2\vec{g})-s(A^{(1)}\partial_{v_1}+A^{(2)}\partial_{v_2})\vec{g}]\\ &=(-A^{(1)}\partial_{v_1}-A^{(2)}\partial_{v_2})[\partial_{v_1}(v_1\vec{g})+\partial_{v_2}(v_2\vec{g})]-s(A^{(1)}\partial_{v_1}+A^{(2)}\partial_{v_2})\partial_s\vec{g}\\ &=(-A^{(1)}\partial_{v_1}-A^{(2)}\partial_{v_2})[\partial_{v_1}(v_1\vec{g})+\partial_{v_2}(v_2\vec{g})-s(A^{(1)}\partial_{v_1}+A^{(2)}\partial_{v_2})\vec{g}]\end{aligned} \tag{3.22}$$

Since the function $\partial_{v_1}(v_1\vec{g})+\partial_{v_2}(v_2\vec{g})-s(A^{(1)}\partial_{v_1}+A^{(2)}\partial_{v_2})\vec{g}$ evaluated at $s=0$ is $\partial_{v_1}(v_1\vec{f})+\partial_{v_2}(v_2\vec{f})$, and it satisfies the hyperbolic system (3.18), we get the conclusion by the definition of $\vec{\mathcal{T}}_{\vec{u}}$ (RHS of (3.19) is just this function evaluated at $s=1$). □

**Theorem 3.2.**

$$\vec{\mathcal{L}}_{\vec{u}}=\vec{\mathcal{T}}_{\vec{u}}\vec{\mathcal{L}}_{\vec{0}}\vec{\mathcal{T}}_{\vec{u}}^{-1}. \tag{3.23}$$

**Proof.** By Lemma 3.1 and the fact that the Laplacian $\Delta_v$ commutes with $\vec{\mathcal{T}}_{\vec{u}}$, one gets

$$\vec{\mathcal{T}}_{\vec{u}}\vec{\mathcal{L}}_{\vec{0}}=\vec{\mathcal{L}}_{\vec{u}}\vec{\mathcal{T}}_{\vec{u}}, \tag{3.24}$$

which is the desired conclusion. □

Define

$$\langle\vec{f},\vec{g}\rangle_{\vec{u}}=\int(\vec{\mathcal{T}}_{\vec{u}}^{-1}\vec{f})\cdot(\vec{\mathcal{T}}_{\vec{u}}^{-1}\vec{g})M_0^{-1}\,\mathrm{d}v, \tag{3.25}$$

where $M_0=\frac{1}{2\pi}\exp(-\frac{|v|^2}{2})$. It is clear that $\langle\vec{f},\vec{f}\rangle_{\vec{u}}$ is positive if $\vec{f}\neq\vec{0}$, and thus $\langle\cdot,\cdot\rangle_{\vec{u}}$ is an inner product on $L^2_{\vec{u}}(\mathbb{R}^2,\mathbb{R}^{K+1})$, defined as the subspace of $L^2(\mathbb{R}^2,\mathbb{R}^{K+1})$ consisting of functions $\vec{f}$ with $\langle\vec{f},\vec{f}\rangle_{\vec{u}}<\infty$. This space is the vector analog of $L^2_u(\mathbb{R}^2)$ defined in Section 2.

From

$$\langle\vec{f},\vec{\mathcal{L}}_{\vec{u}}\vec{g}\rangle_{\vec{u}}=\int\vec{\mathcal{T}}_{\vec{u}}^{-1}\vec{f}\cdot(\vec{\mathcal{T}}_{\vec{u}}^{-1}\vec{\mathcal{L}}_{\vec{u}}\vec{g})M_0^{-1}\,\mathrm{d}v=\int\vec{\mathcal{T}}_{\vec{u}}^{-1}\vec{f}\cdot(\vec{\mathcal{L}}_{\vec{0}}\vec{\mathcal{T}}_{\vec{u}}^{-1}\vec{g})M_0^{-1}\,\mathrm{d}v, \tag{3.26}$$

and the self-adjointness of $\mathcal{L}_0$, it is clear that $\vec{\mathcal{L}}_{\vec{u}}$ is self-adjoint on $L^2_{\vec{u}}(\mathbb{R}^2,\mathbb{R}^{K+1})$. Also, it follows from (2.4) that

$$\langle\vec{f},\vec{\mathcal{L}}_{\vec{u}}\vec{f}\rangle_{\vec{u}}=\int\vec{\mathcal{T}}_{\vec{u}}^{-1}\vec{f}\cdot(\vec{\mathcal{L}}_{\vec{0}}\vec{\mathcal{T}}_{\vec{u}}^{-1}\vec{f})M_0^{-1}\,\mathrm{d}v=-\int M_0\left|\nabla_v\left(\frac{\vec{\mathcal{T}}_{\vec{u}}^{-1}\vec{f}}{M_0}\right)\right|^2\mathrm{d}v\le 0, \tag{3.27}$$

which is a vector analog of the coercivity estimate (2.4). From (3.27) it is easy to prove the following theorem:

**Theorem 3.3.** *The null space of $\vec{\mathcal{L}}_{\vec{u}}$ is given by*

$$\vec{M}(v)=\vec{\mathcal{T}}_{\vec{u}}(M_0\vec{C}), \tag{3.28}$$

*where $M_0=\frac{1}{2\pi}\exp(-\frac{|v|^2}{2})$, and $\vec{C}$ is any constant vector.*

### 3.4. The hydrodynamic limit of the gPC system

Based on Theorem 3.3, we formally derive the hydrodynamic limit of the gPC system (3.14), and show that the limit is the gPC approximation to the limiting Navier–Stokes system (2.9), which means that the gPC approximation (3.14) is s-AP.

Define the moments of $\vec{f}$ by

$$\vec{n} = \int \vec{f}\,\mathrm{d}v, \quad \vec{J} = \int v\vec{f}\,\mathrm{d}v, \quad \vec{P} = \int v \otimes v\vec{f}\,\mathrm{d}v. \tag{3.29}$$

As $\epsilon \to 0$, from (3.14) one formally has $\vec{\mathcal{L}}_{\vec{u}}\vec{f} = 0$, which implies

$$\vec{f}(v) = \vec{M}(v) = \vec{\mathcal{T}}_{\vec{u}}(M_0\vec{C}), \tag{3.30}$$

by Theorem 3.3. Substituting into (3.29), one gets

$$\begin{aligned}
&\vec{n} = \int \vec{M}(v)\,\mathrm{d}v = \vec{C},\\
&\vec{J}^{(i)} = \int v_i\vec{M}(v)\,\mathrm{d}v = A^{(i)}\vec{n}, \quad i = 1,2,\\
&\vec{P}^{(ij)} = \int v_i v_j\vec{M}(v)\,\mathrm{d}v = \delta_{ij}\vec{n} + \frac{1}{2}(A^{(i)}A^{(j)} + A^{(j)}A^{(i)})\vec{n}, \quad i,j = 1,2,
\end{aligned} \tag{3.31}$$

which are consistent with the expression of $J, P$ in the deterministic case (see (2.6)). Integrating the first equation of (3.14) against $1, v$ one gets

$$\begin{cases}
\partial_t\vec{n} + \nabla_x\cdot\vec{J} = 0,\\
\partial_t\vec{J}^{(i)} + \nabla_x\cdot\vec{P}^{(i)} - \vec{n}\nabla_{x_i}\Phi = -\dfrac{1}{\epsilon}\displaystyle\int (v_i - A^{(i)})\vec{f}\,\mathrm{d}v, \quad i = 1,2.
\end{cases} \tag{3.32}$$

Substituting (3.31) into the above equations and doing proper linear combinations, one has

$$\begin{cases}
\partial_t\vec{n} + \nabla_x\cdot(A\vec{n}) = 0,\\
\partial_t(\vec{u}^{(i)} + \kappa A^{(i)}\vec{n}) + \nabla_x\cdot[A\vec{u}^{(i)} + \dfrac{\kappa}{2}(A^{(i)}A + AA^{(i)})\vec{n}]\\
\qquad + \partial_{x_i}(\vec{p} + \kappa\vec{n}) + \kappa\vec{n}\partial_{x_i}\Phi = \dfrac{1}{Re}\Delta_x\vec{u}^{(i)}, \quad i = 1,2.
\end{cases} \tag{3.33}$$

Note if one inserts the gPC ansatz (3.10) and (3.11) with definitions in (3.29) into the Navier–Stokes system (2.9) and conducts the Galerkin projection, one gets exactly (3.33). Thus the s-AP property of (3.14) is justified.

## 4. The fully discrete s-AP scheme for the system with uncertainty

For simplicity of notation, in this section, an expression of the form $c + B$ where $c$ is a scalar and $B$ is a matrix is interpreted as $cI + B$, where $I$ is the identity matrix.

In order to get a first order AP scheme for the system with uncertainty, we follow the steps of the deterministic AP scheme [13]. Starting from (3.14), we first give an outline of the scheme, and then provide justifications in the subsequent sections.

STEP 1: Integrating the first equation of (3.14) over $v$,

$$\frac{1}{\Delta t}(\vec{n}^{k+1} - \vec{n}^k) = -\int v\cdot\nabla_x\vec{f}^k\,\mathrm{d}v. \tag{4.1}$$

Then one gets $\vec{n}^{k+1}$.

STEP 2: We adopt the idea of the projection method for the Navier–Stokes equations. We first solve the second equation of (3.14) with the pressure term being $\nabla_x\vec{p}^k$, and then solve for the increment of $\vec{p}$. Multiplying the first equation of (3.14) and integrating over $v$, combining with the second equation of (3.14), one gets

$$\frac{1}{\Delta t}(\vec{J}^* - \vec{J}^k) = -\int v\otimes v\cdot\nabla_x\vec{f}^k\,\mathrm{d}v - \vec{n}^k\nabla_x\Phi - \frac{1-\alpha}{\epsilon}[\vec{J}^* - A(\vec{n}^{k+1})\vec{u}^*], \tag{4.2}$$

$$\frac{1}{\Delta t}(\vec{u}^* - \vec{u}^k) + \nabla_x\vec{p}^k - \Delta_x\vec{u}^* = -\nabla_x\cdot[A(\vec{u}^k)\otimes\vec{u}^k] + \frac{1-\alpha}{\epsilon}\kappa[\vec{J}^* - A(\vec{n}^{k+1})\vec{u}^*], \tag{4.3}$$

where $\alpha \in (0,1)$ is a fixed parameter to be chosen. Only a part of the stiff term $\frac{1-\alpha}{\epsilon}(\vec{J}^* - A(\vec{n}^{k+1})\vec{u}^*)$ is contained in this step, and another part is contained in STEP 3. The purpose of this is to make sure that as $\epsilon \to 0$, the equation $\vec{J} = A(\vec{n})\vec{u}$ holds at each step. Eliminating $\vec{J}^*$ one gets,

$$\begin{aligned}(B_1 - \frac{1}{Re}\Delta_x)\vec{u}^* = \frac{\vec{u}^k}{\Delta t} - \nabla_x \cdot [A(\vec{u}^k)\otimes \vec{u}^k] \\ - \nabla_x \vec{p}^k + \frac{(1-\alpha)\kappa}{\epsilon + (1-\alpha)\Delta t}(\vec{J}^k - \Delta t \int v \otimes v \nabla_x \vec{f}^k \, \mathrm{d}v - \Delta t \vec{n}^k \nabla_x \Phi),\end{aligned} \tag{4.4}$$

where

$$B_1 = \frac{1}{\Delta t} + \frac{1-\alpha}{\epsilon + (1-\alpha)\Delta t}\kappa A(\vec{n}^{k+1}). \tag{4.5}$$

This is a system of the Helmholtz equation, whose coefficient matrix $B_1$ is symmetric positive definite under reasonable and mild assumptions on $\vec{n}^{k+1}$ (given in Section 4.1). Solving it by the conjugate gradient method to get $\vec{u}^*$, and then substituting the result of $\vec{u}^*$ into (4.2), one gets $\vec{J}^*$.

STEP 3: To solve for the increment of $\vec{p}$, make $\vec{u}^{k+1}$ divergence-free, and include the other part of the stiff term $\frac{\alpha}{\epsilon}(\vec{J}^{**} - A(\vec{n}^{k+1})\vec{u}^{k+1})$, one has

$$\begin{aligned}&\frac{1}{\Delta t}(\vec{J}^{**} - \vec{J}^*) = -\frac{\alpha}{\epsilon}[\vec{J}^{**} - A(\vec{n}^{k+1})\vec{u}^{k+1}], \\ &\frac{1}{\Delta t}(\vec{u}^{k+1} - \vec{u}^*) + \nabla_x(\vec{p}^{k+1} - \vec{p}^k) = \frac{\alpha}{\epsilon}\kappa[\vec{J}^{**} - A(\vec{n}^{k+1})\vec{u}^{k+1}].\end{aligned} \tag{4.6}$$

Eliminate $J^{**}$,

$$\begin{aligned}&\vec{u}^{k+1} + \left[\frac{1}{\Delta t} + \frac{\alpha}{\epsilon}(1 + \kappa A(\vec{n}^{k+1}))\right]^{-1}(\frac{1}{\Delta t} + \frac{\alpha}{\epsilon})\Delta t \nabla_x(\vec{p}^{k+1} - \vec{p}^k) \\ &= \left[\frac{1}{\Delta t} + \frac{\alpha}{\epsilon}(1 + \kappa A(\vec{n}^{k+1}))\right]^{-1}\left((\frac{1}{\Delta t} + \frac{\alpha}{\epsilon})\vec{u}^* + \frac{\alpha}{\epsilon}\kappa \vec{J}^*\right).\end{aligned} \tag{4.7}$$

To solve for $\vec{u}^{k+1}$, first take divergence:

$$\nabla_x \cdot (B_2 \nabla_x (p^{k+1} - p^k)) = \frac{1}{\Delta t}\nabla_x \cdot \left[\left[\frac{1}{\Delta t} + \frac{\alpha}{\epsilon}(1 + \kappa A(\vec{n}^{k+1}))\right]^{-1}\left((\frac{1}{\Delta t} + \frac{\alpha}{\epsilon})\vec{u}^* + \frac{\alpha}{\epsilon}\kappa \vec{J}^*\right)\right], \tag{4.8}$$

with

$$B_2 = \left[\frac{1}{\Delta t} + \frac{\alpha}{\epsilon}(1 + \kappa A(\vec{n}^{k+1}))\right]^{-1}(\frac{1}{\Delta t} + \frac{\alpha}{\epsilon}). \tag{4.9}$$

This is a system of the variable coefficient Poisson equation for $(\vec{p}^{k+1} - \vec{p}^k)$, whose coefficient matrix is symmetric positive definite under reasonable assumptions on $\vec{n}^{k+1}$ (given in Section 4.1). Solving it with the Neumann boundary condition

$$\left.\frac{\partial(\vec{p}^{k+1} - \vec{p}^k)}{\partial v}\right|_{\partial\Omega} = 0, \tag{4.10}$$

by the conjugate gradient method to get $\vec{p}^{k+1}$, and then substituting back to (4.7), one gets $\vec{u}^{k+1}$.

STEP 4: To get $\vec{f}^{k+1}$ we solve the first equation of (3.14) with the stiff term $\vec{\mathcal{L}}_{\vec{u}}\vec{f}$ treated implicitly, using the $\vec{u}^{k+1}$ obtained above:

$$\frac{\vec{f}^{k+1} - \vec{f}^k}{\Delta t} + v \cdot \nabla_x \vec{f}^k - \nabla_x \Phi \cdot \nabla_v \vec{f}^k = \frac{1}{\epsilon}\vec{\mathcal{L}}_{\vec{u}^{k+1}}\vec{f}^{k+1}. \tag{4.11}$$

Using the relation $\vec{\mathcal{L}}_{\vec{u}} = \vec{\mathcal{T}}_{\vec{u}}\vec{\mathcal{L}}_{\vec{0}}\vec{\mathcal{T}}_{\vec{u}}^{-1}$ (where we omit the index $k+1$ on $\vec{u}$), one gets

$$\vec{f}^{k+1} = \epsilon \vec{\mathcal{T}}_{\vec{u}}(\frac{\epsilon}{\Delta t} - \vec{\mathcal{L}}_{\vec{0}})^{-1}\vec{\mathcal{T}}_{\vec{u}}^{-1}\left(\frac{\vec{f}^k}{\Delta t} - v \cdot \nabla_x \vec{f}^k + \nabla_x \Phi \cdot \nabla_v \vec{f}^k\right). \tag{4.12}$$

The computation of the operator $\vec{\mathcal{T}}_{\vec{u}}$ and $\vec{\mathcal{T}}_{\vec{u}}^{-1}$ is given in Section 4.2, and the inversion of $(\frac{\epsilon}{\Delta t} - \vec{\mathcal{L}}_{\vec{0}})$ can be done by the same method as the deterministic case [19] (see the Appendix for details), since $\vec{\mathcal{L}}_{\vec{0}}$ is the operator $\mathcal{L}_0$ acting on each gPC mode. Thus one can get $\vec{f}^{k+1}$, and get $\vec{J}^{k+1}$ by taking moments of $\vec{f}^{k+1}$.

The second order AP scheme can be derived in the same way as the deterministic case, see [13] for details.

### 4.1. On the Helmholtz equation and the Poisson equation

In STEP 2 and STEP 3 one needs to solve a system of Helmholtz equations and a system of Poisson equations respectively. We give the proof of positive definiteness of the coefficient matrices of these equations under reasonable assumptions.

In STEP 2 the system of Helmholtz equations for $\vec{u}^*$ has the form (we omit the time step indexes)

$$(B_1 - \frac{1}{Re}\Delta_x)\vec{u}(x) = \vec{g}(x), \tag{4.13}$$

where $B_1$ is defined in (4.5). Define the LHS of (4.13) as $\mathcal{B}_1(\vec{u})$, and then $\mathcal{B}_1$ is an (unbounded) operator on the Hilbert space $L^2(\Omega, \mathbb{R}^{K+1})$. $\mathcal{B}_1$ is symmetric since

$$\begin{aligned}
&< \mathcal{B}_1(\vec{u}), \vec{w} > \\
&= \int \left[ \sum_{i,j,k=0}^{K} \frac{1-\alpha}{\epsilon + (1-\alpha)\Delta t} S_{ijk} n_i(x) u_j(x) + \sum_{k=0}^{K} (\frac{1}{\Delta t} - \frac{1}{Re}\Delta_x u_k(x)) \right] w_k(x)\, dx \\
&= \int \sum_{k=0}^{K} \left( \frac{1}{\Delta t} u_k(x) w_k(x) + \frac{1}{Re} \nabla_x u_k(x) \cdot \nabla_x w_k(x) \right) dx \\
&\qquad + \frac{1-\alpha}{\epsilon + (1-\alpha)\Delta t} \int \int n^K(x,z) u^K(x,z) w^K(x,z) \pi(z)\, dz\, dx
\end{aligned} \tag{4.14}$$

for $\vec{u}, \vec{w} \in H_0^1(\Omega, \mathbb{R}^{K+1})$.

By Poincaré's Inequality,

$$\int |\nabla u_k(x)|^2\, dx \geq C_1 \int |u_k(x)|^2\, dx, \tag{4.15}$$

for some positive constant $C_1$ depending on $\Omega$, the $x$-domain. Then, under the assumption that

$$n^K(x,z) > -\delta_1, \tag{4.16}$$

where

$$\delta_1 = \frac{(1 + C_1 \Delta t/Re)(\epsilon + (1-\alpha)\Delta t)}{(1-\alpha)\Delta t} > 1, \tag{4.17}$$

one can see that $\mathcal{B}_1$ is positive definite. The assumption (4.16) is reasonable since $n^K(x,z)$ is an approximation of $n(x,z) \geq 0$ with a spectral accuracy (see Remark 4.1 for more details).

In STEP 3 the system of Poisson equations for $\vec{u}^{**}$ has the form

$$\nabla \cdot (B_2 \nabla \vec{u}(x)) = \vec{g}(x), \tag{4.18}$$

where $B_2$ is defined in (4.9). Define the LHS as $\mathcal{B}_2(\vec{u})$, and then $\mathcal{B}_2$ is an (unbounded) operator on the Hilbert space $L^2(\Omega, \mathbb{R}^{K+1})$. $\mathcal{B}$ is symmetric since

$$\begin{aligned}
&< \mathcal{B}_2(\vec{u}), \vec{w} > \\
&= \int \sum_{j,k=0}^{K} (\nabla_x \cdot (B_{2,jk}(x) \nabla u_j(x)) w_k(x))\, dx \\
&= -\int \sum_{j,k=0}^{K} B_{2,jk}(x) \nabla_x u_j(x) \cdot \nabla_x w_k(x)\, dx
\end{aligned}$$

for $\vec{u}, \vec{w} \in H_0^1(\Omega, \mathbb{R}^{K+1})$. Similar to the case of $\mathcal{B}_1$, one can show that the matrix $\left[ \frac{1}{\Delta t} + \frac{\alpha}{\epsilon}(1 + \kappa A(\vec{n})) \right]$ is positive definite if

$$n^K(x,z) > -\delta_2, \tag{4.19}$$

where

$$\delta_2 = \frac{\epsilon + \alpha \Delta t}{\alpha \kappa \Delta t} > \frac{1}{\kappa}. \tag{4.20}$$

This assumption is also reasonable due to the positivity of the exact solution $n(x,z)$ (see Remark 4.1 for more details). Then one can deduce that the inverse matrix in the definition of $B_2$ exists, and $B_2$ is also positive definite. Therefore the operator $\mathcal{B}_2$ is negative definite.

**Remark 4.1.** In general the numerical solution $n^K(x,z)$ is not necessarily positive everywhere. However, since the exact solution $n(x,z)$ is positive everywhere, and the gPC approximation is spectrally accurate (based on the smoothness of $n(x,z)$), it is expected that (4.16) and (4.19) are easily satisfied if $K$ is reasonably large.

The loss of positivity is a pitfall of any spectral method, with no exception to the gPC method. We did not encounter any problem in this paper. If positivity is necessary (for example, if one considers a more complicated model where $n$ enters into the definition of drag coefficients), one might need to use some positivity-preserving techniques, such as the one developed in [32], to fix the problem. This will be studied in a subsequent work.

### 4.2. Computing $\vec{\mathcal{T}}$ numerically

In STEP 4 it is required to compute the operator $\vec{\mathcal{T}}_{\vec{u}} = \exp(-A^{(1)}\partial_{v_1} - A^{(2)}\partial_{v_2})$. If one computes it directly by the discrete Fourier transform, then one needs to multiply $\exp(-iA^{(1)}\xi_1 - iA^{(2)}\xi_2)$ on each Fourier mode $(\xi_1,\xi_2)$. Since the matrices $A^{(1)}$ and $A^{(2)}$ do not commute in general, in order to compute these matrix exponentials, one has to diagonalize the matrix $(A^{(1)}\xi_1 + A^{(2)}\xi_2)$ for each $(\xi_1,\xi_2)$. Thus one needs $N_v^2$ times of diagonalization of matrices of size $K+1$, where $N_v$ is the number of mesh points in one dimension of the velocity space. This can be extremely expensive if $N_v$ and $K$ are large. Here we introduce an operator splitting

$$\exp(-A^{(1)}\partial_{v_1} - A^{(2)}\partial_{v_2})\vec{f} \approx \exp(-A^{(1)}\partial_{v_1})\exp(-A^{(2)}\partial_{v_2})\vec{f}. \tag{4.21}$$

In general, on the Fourier mode $(\xi_1,\xi_2)$, the difference between the matrices $\exp(-iA^{(1)}\xi_1 - iA^{(2)}\xi_2)$ and $\exp(-iA^{(1)}\xi_1)\times \exp(-iA^{(2)}\xi_2)$ can be of order $O(1)$ since the commutator of $A^{(1)}$ and $A^{(2)}$ can be of order $O(1)$. However, we will prove that under smoothness assumptions, the splitting (4.21) has spectral accuracy and show that it saves the computational cost of $\vec{\mathcal{T}}_{\vec{u}}$ dramatically. By saying that an approximation has *spectral accuracy*, or an error is *spectrally small*, we mean that the error of the approximation in $L^2$ norm is less than $\frac{C_m}{K^m}$, for any $m \geq 1$. Our accuracy result is

**Theorem 4.2.** *Assume that $u(z) = u^K$ is sufficiently smooth in $z$, $f(v,z) = f^K$ is sufficiently smooth in $v, z$. Then the splitting (4.21) has spectral accuracy, namely,*

$$\exp(-A^{(1)}\partial_{v_1} - A^{(2)}\partial_{v_2})\vec{f} - \exp(-A^{(1)}\partial_{v_1})\exp(-A^{(2)}\partial_{v_2})\vec{f} = O(\frac{1}{K^m}), \quad \forall m \geq 1, \tag{4.22}$$

*where $m$ depends on the regularity of $u$ and $f$.*

To prove the theorem, we need the following lemma concerning the spectral accuracy of the gPC approximation of the linear transport equation:

**Lemma 4.3.** *Consider the equation*

$$\partial_s g + u\cdot\nabla_v g = 0, \quad g|_{s=0} = g^0, \tag{4.23}$$

*where $g = g(s,v,z)$, $u(z) = u^K(z)$, and its gPC approximation*

$$\partial_s \tilde{g} + A(u)\cdot\nabla_v \tilde{g} = 0, \quad \tilde{g}|_{s=0} = (g^0)^K, \tag{4.24}$$

*where the matrix $A(u)$ acts on $\tilde{g}$ by matrix multiplication as if $\tilde{g}$ is written in the vector form $\vec{g}$ (see (3.13)). Suppose $u$ is sufficiently smooth in $z$ and $g^0$ is sufficiently smooth in $v, z$. Then $\tilde{g}|_{s=1}$ as an approximation of $g|_{s=1}$ has spectral accuracy.*

**Proof.** Denote $P_K$ as the projection onto the gPC approximation space. Then $P_K g$ satisfies

$$\partial_s P_K g + P_K(u\cdot\nabla_v P_K g) + P_K(u\cdot\nabla_v(I-P_K)g) = 0. \tag{4.25}$$

By the definition of $A(u)$ in (3.13), one can see that

$$A(u)\cdot\nabla_v\tilde{g} = P_K(u\cdot\nabla_v\tilde{g}). \tag{4.26}$$

Thus

$$\partial_s\tilde{g} + P_K(u\cdot\nabla_v\tilde{g}) = 0. \tag{4.27}$$

Take the difference between (4.25) and (4.27) one gets

$$\partial_s(P_K g - \tilde{g}) + A(u)\cdot\nabla_v(P_K g - \tilde{g}) + P_K(u\cdot\nabla_v(I-P_K)g) = 0. \tag{4.28}$$

Since $P_K g = \tilde{g} = (g^0)^K$ at $s = 0$, one solves the above equation as

$$(P_K g - \tilde{g})|_{s=1} = -\int_0^1 \exp(-(1-\tau)A(u)\cdot\nabla_v) P_K (u\cdot\nabla_v (I-P_K) g(\tau, v, z))\, \mathrm{d}\tau. \tag{4.29}$$

Since $g(s, v, z) = g^0(v - su(z), z)$ and $g^0, u$ are sufficiently smooth, the higher order $v, z$-derivatives of $g$ are bounded in $L^\infty_s([0,1], L^2_{v,z})$. Thus $\nabla_v (I - P_K)g$ is spectrally small in the same norm, and so is $P_K(u\cdot\nabla_v(I-P_K)g)$. Since $\exp(-(1-\tau)A(u)\cdot\nabla_v)$ is unitary, one concludes that $(P_K g - \tilde{g})|_{s=1}$ is spectrally small. Then one can get the conclusion since $(P_K g - g)|_{s=1}$ is spectrally small due to the smoothness of $g|_{s=1}$. □

**Proof of Theorem 4.2.** One notes that the previous lemma implies that

$$\exp(-A^{(1)}\partial_{v_1} - A^{(2)}\partial_{v_2})\vec{f} - f^K(v - u(z), z) \tag{4.30}$$

is spectrally small, where the first term is interpreted as a function of $v, z$. Also, by taking $u = (0, u^{(2)})$, the lemma implies that

$$\exp(-A^{(2)}\partial_{v_2})\vec{f} - f^K(v_1, v_2 - u^{(2)}(z), z) \tag{4.31}$$

is spectrally small. Then, by taking $u = (u^{(1)}, 0)$, the lemma implies that

$$\exp(-A^{(1)}\partial_{v_1})\exp(-A^{(2)}\partial_{v_2})\vec{f} - f^K(v_1 - u^{(1)}(z), v_2 - u^{(2)}(z), z) \tag{4.32}$$

is spectrally small. Then combining (4.30) and (4.32) the theorem is proved. □

Thus if one computes $\vec{\mathcal{T}}_{\vec{u}}$ by the RHS of (4.21), then at most a spectral error is introduced. The RHS of (4.21) can be computed by using the discrete Fourier transform. For example, the operator $\exp(-A^{(1)}\partial_{v_1})$ is the multiplication of $\exp(-iA^{(1)}\xi_1)$ on the Fourier mode $\xi_1$. By diagonalizing the matrix $A^{(1)}$, all such matrix exponentials are easily computed. Thus, with this splitting, *only two* (instead of $N_v^2$ as in the direct method) matrix diagonalizations are required.

## 5. Numerical results

In the numerical tests in this section, the $x$-domain is $[0,1]\times[0,1]$, and the no-slip boundary condition for $u$ is taken. We take the parameters $\kappa = 2$, $Re = 1000$, and $\Phi(x) = x_2$ the gravity field. The random domain is taken as $I_z = [-1, 1]$ with the uniform distribution, except for the last example, where $I_z = (-\infty, \infty)$ with the normal distribution $\mathcal{N}(0,1)$. For the stochastic Galerkin method, we take

$$K = 6, \quad N_x = 128, \quad N_v = 32, \quad R_v = 7, \quad \Delta t = 1/2560. \tag{5.1}$$

The mesh sizes are given by

$$\Delta x = \frac{1}{N_x}, \quad \Delta v = \frac{2R_v}{N_v}. \tag{5.2}$$

The $\Delta t$ is about $0.18\frac{\Delta x}{R_v}$, which satisfies the CFL condition for the kinetic flux term $v\cdot\nabla_x f$. For the problems in subsection 5.2, the total time $t$ is taken as 2000 time steps, which is about $t = 0.39$.

The mesh points of the $x$-domain and the $v$-domain are defined by

$$\begin{aligned} x_{i,j} &= \left((i+\frac{1}{2})\Delta x, (j+\frac{1}{2})\Delta x\right), \quad i, j = 0, \dots, N_x - 1 \\ v_{i,j} &= \left(-R_v + (i+\frac{1}{2})\Delta v, -R_v + (j+\frac{1}{2})\Delta v\right), \quad i, j = 0, \dots, N_v - 1 \end{aligned} \tag{5.3}$$

The kinetic flux term $v\cdot\nabla_x f$ and the forcing term $\nabla_x\Phi\cdot\nabla_v f$ are numerically approximated by the second order upwind scheme with the minmod slope limiter. Other flux terms are approximated by the centered difference scheme.

Given a function $g(z) = \sum_{k=0}^K g_k\phi_k(z)$, the expectation value is given by $g_0$ and the standard deviation is given by $\sqrt{\sum_{k=1}^K g_k^2}$.

Given the bulk density $n(z) = \sum_{k=0}^K n_k\Phi_k(z)$ and the momentum $J(z) = \sum_{k=0}^K J_k\Phi_k(z)$ of the particles, the bulk velocity of the particles $u^p(z) \approx \sum_{k=0}^K u_k^p\Phi_k(z)$ is computed by solving $u_k^p$ from the linear equations

$$A(n)\vec{u^p} = \vec{J}, \tag{5.4}$$

where $A(n)$ is defined in (3.13). It is easy to check that the matrix $A(n)$ is symmetric positive-definite if $n(z)$ is everywhere positive. Thus $\vec{u^p}$ can be solved from this set of linear equations. In all the numerical experiments we conducted in this paper, $A(n)$ is always invertible. However, the gPC method does not guarantee positivity. To deal with the positivity issue, see discussions in Remark 4.1.

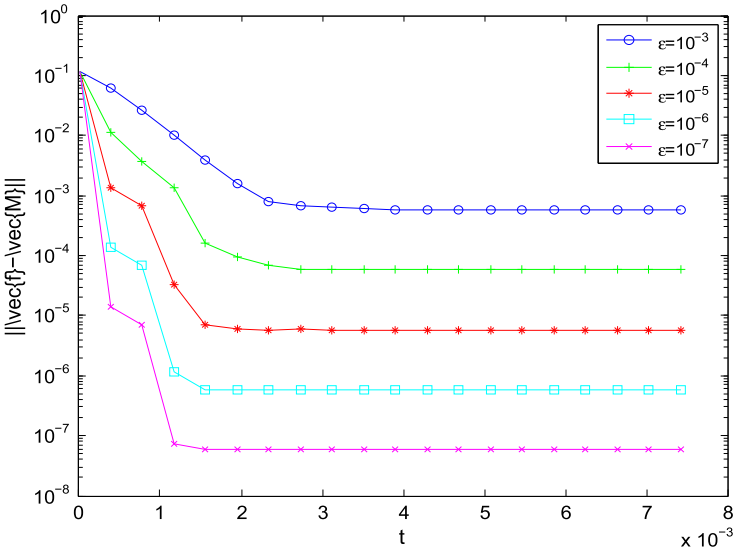


**Fig. 1.** The s-AP property: time evolution of $\|\vec{f}-\vec{M}\|$ measured in $L^\infty_x(L^2_{v,z})$, $\epsilon = 10^{-3}, 10^{-4}, 10^{-5}, 10^{-6}, 10^{-7}$.

### 5.1. The s-AP property

To verify the s-AP property of the stochastic Galerkin method, we take initial fluid velocity

$$u = (x_2 - 0.5, -(x_1 - 0.5)) \cdot 1000(1 + 0.2z) \cdot [(x_1 - 0.5)^2 + (x_2 - 0.5)^2] \cdot \exp[-100((x_1 - 0.5)^2 + (x_2 - 0.5)^2)], \tag{5.5}$$

and particle distribution as the Maxwellian with density

$$n = 0.5 - 0.4 \arctan[10(x_1 - 0.5)]/(\pi/2), \tag{5.6}$$

and bulk velocity $\frac{J}{n} = -u$. Notice that this is different from the equilibrium, which is given by a Maxwellian with bulk velocity $u$. We observe the time evolution of the difference between $\vec{f}$ and the corresponding equilibrium $\vec{M} = \vec{\mathcal{T}}_{\vec{u}}(M_0\vec{n})$ with $\vec{n} = \int \vec{f}\, dv$ for different values of $\epsilon$ (see Section 3.3 for related definitions). The difference is measured in $L^\infty_x(L^2_{v,z})$. The result is shown in Fig. 1. One can clearly see that $\vec{f}$ is driven to $\vec{M}$ as $t$ increases, until $\|\vec{f} - \vec{M}\| = O(\epsilon)$.

### 5.2. Problems with random initial data

#### 5.2.1. Example 1: random initial fluid velocity

We take the initial fluid velocity the same as (5.5) and the particle distribution as the equilibrium with density as in (5.6) and bulk velocity the same as the fluid velocity. With this initial data, the fluid near the center of the domain is rotating clockwisely, and the particle density has the tendency of falling to the left bottom due to gravity, as well as the tendency of diffusion due to the gradient of the density.

The expectation and standard deviation of the fluid velocity $u$ and the macroscopic quantities of the particles are shown in Figs. 2, 3, 4 (for $\epsilon = 1, 0.01, 10^{-8}$ respectively).

One can clearly see that for $\epsilon = 1$, the fluid velocity and the particle bulk velocity differ much. From the expectations of $n$ and $u^p$ one can clearly see that the particles are falling down (second component of $u^p$) and there is a strong diffusion of the particles due to the gradient of the initial density (first component of $u^p$). The randomness on the initial bulk velocity and fluid velocity have little effect on the particle density and bulk velocity afterwards.

For $\epsilon = 0.01$ the fluid velocity and the particle bulk velocity are very close but not the same; for $\epsilon = 10^{-8}$ they look the same. Also, in these two cases one can clearly see that the fluid together with the particles are rotating clockwisely, while for $\epsilon = 0.01$ there is still some visible kinetic effect which is smoothing, compared to the $\epsilon = 10^{-8}$ case. The s-AP property is verified because (1) smaller $\epsilon$ makes the fluid velocity and the particle bulk velocity closer, (2) the solution with $\epsilon = 0.01$ is close to the solution with $\epsilon = 10^{-8}$, which can be viewed as the solution of the limiting system since $\epsilon << \Delta t, \Delta x$.

One can also see that in all three cases, the fluid velocity is sensitive to the initial uncertainty, while for the particle density and bulk velocity, they are insensitive to the initial uncertainty for $\epsilon = 1$ case, and sensitive for the $\epsilon = 0.01$, $10^{-8}$ cases. The reason for the insensitiveness in the kinetic regime is that the interaction between the particles and the fluid is weak, and the kinetic diffusion effect and the gravity dominate the motion of the particles.

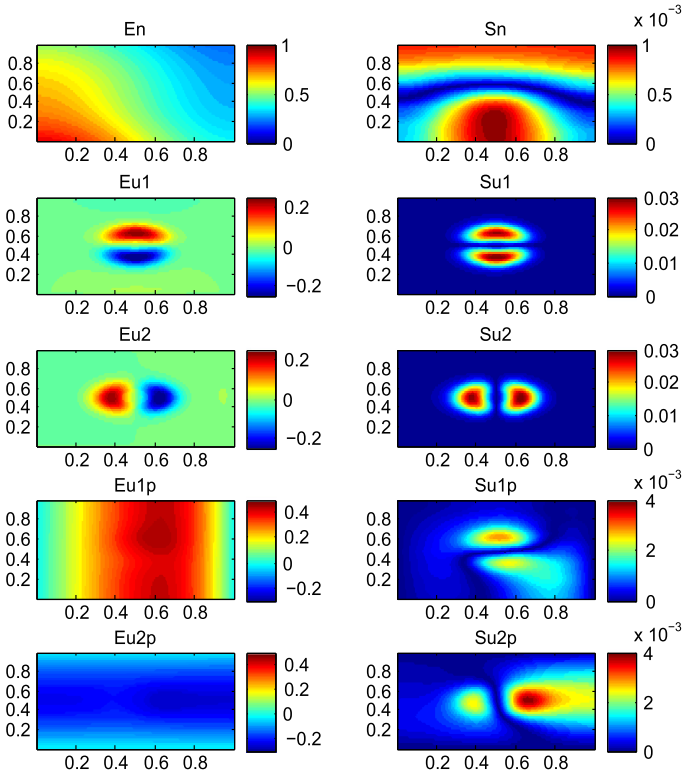


**Fig. 2.** Example 1: $\epsilon = 1$. Left column: expectation. Right column: standard deviation. Rows: particle density $n$, fluid velocity $u$ (two components), particle bulk velocity $\frac{J}{n}$ (two components).

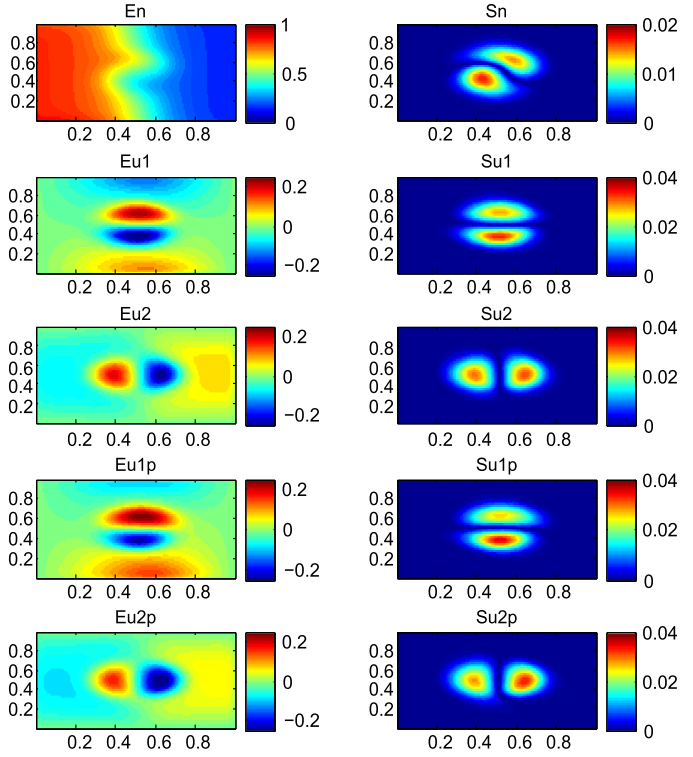


**Fig. 3.** Example 1: $\epsilon = 0.01$. Left column: expectation. Right column: standard deviation. Rows: particle density $n$, fluid velocity $u$ (two components), particle bulk velocity $\frac{J}{n}$ (two components).

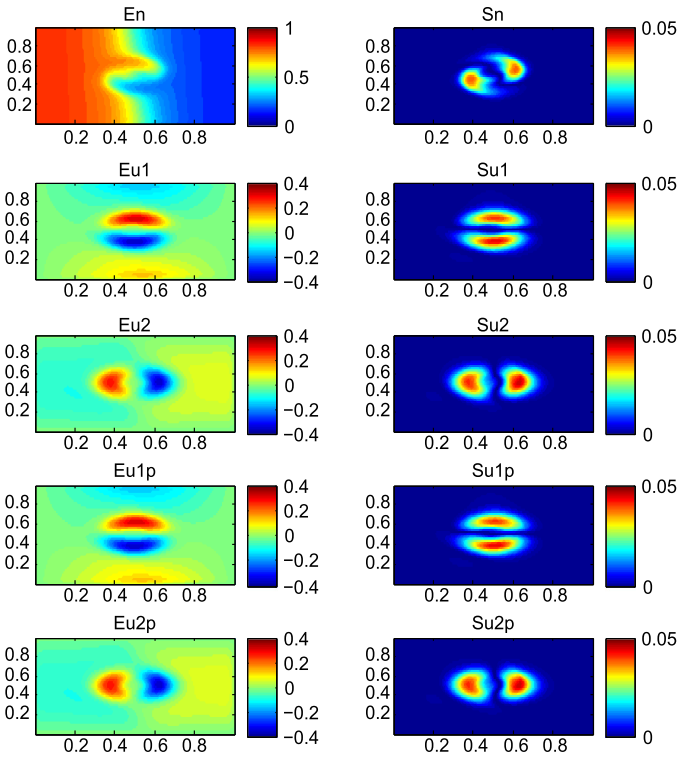


**Fig. 4.** Example 1: $\epsilon = 10^{-8}$. Left column: expectation. Right column: standard deviation. Rows: particle density $n$, fluid velocity $u$ (two components), particle bulk velocity $\frac{J}{n}$ (two components).

We also compare the solution by the stochastic Galerkin method with the solution by a stochastic collocation (sC) method with 10 Gauss–Legendre collocation points. The results are compared at the 1d slice $x_1 = 0.55$ and shown in Fig. 5.

One can see that the expectations computed by the two methods agree very well, while some standard deviations have some discrepancy due to their small magnitude.

To compare the efficiency of the sG method and the sC method, since the exact solution is expected to be smooth, one expects that the sG method with degree $K$ polynomials will give the same accuracy as the Gauss–Legendre sC method with $K$ collocation points in each random direction. Since the sC method is non-intrusive, one expects that for 1d random space sC is more efficient than sG. However, if one considers a $d$-dimensional random space, then sG requires $\binom{K+d}{d}$ basis functions, while sC with tensor grids requires $K^d$ collocation points. From this one can see that sG can be much more efficient than sC if $d$ is large. However, to seriously compare the efficiency of the two methods in very high dimension, one needs to utilize sparse grids in both methods. This is out of the scope of the paper.

*5.2.2. Example 2: random initial particle density*

We take initial fluid velocity as zero and particle distribution as the equilibrium with density

$$n = 0.5 - 0.4 \arctan[10(x_1 - 0.5 + 0.1z + 0.2x_2)]/(\pi/2), \tag{5.7}$$

and bulk velocity as zero. The particles still tend to fall to left bottom, and diffuse, and as a result, the fluid will be forced to rotate counter-clockwisely.

The expectation and standard deviation of the fluid velocity and the macroscopic quantities of the particles are shown in Figs. 6, 7, 8 (for $\epsilon = 1, 0.01, 10^{-8}$ respectively).

For $\epsilon = 1$ one can see the expected behavior of the particles, as well as the rotation of the fluid. Notice that the fluid velocity is much smaller than the particle bulk velocity, and their shapes do not look similar. This is because for $\epsilon = 1$ the interaction between the fluid and the particles is weak. Also one can see the randomness on the initial density propagates into the particle bulk velocity and the fluid velocity.

As $\epsilon$ getting smaller, one can clearly see that the fluid velocity and the particle bulk velocity get closer, and they are rotating counter-clockwisely. Also, the solution with $\epsilon = 0.01$ is close to the solution with $\epsilon = 10^{-8}$. This verifies the s-AP property.

In all three cases, the particle density and bulk velocity are sensitive to the initial uncertainty, while the fluid velocity becomes sensitive only when $\epsilon$ gets small ($\epsilon = 0.01, 10^{-8}$). This is because there is no uncertainty in the initial fluid

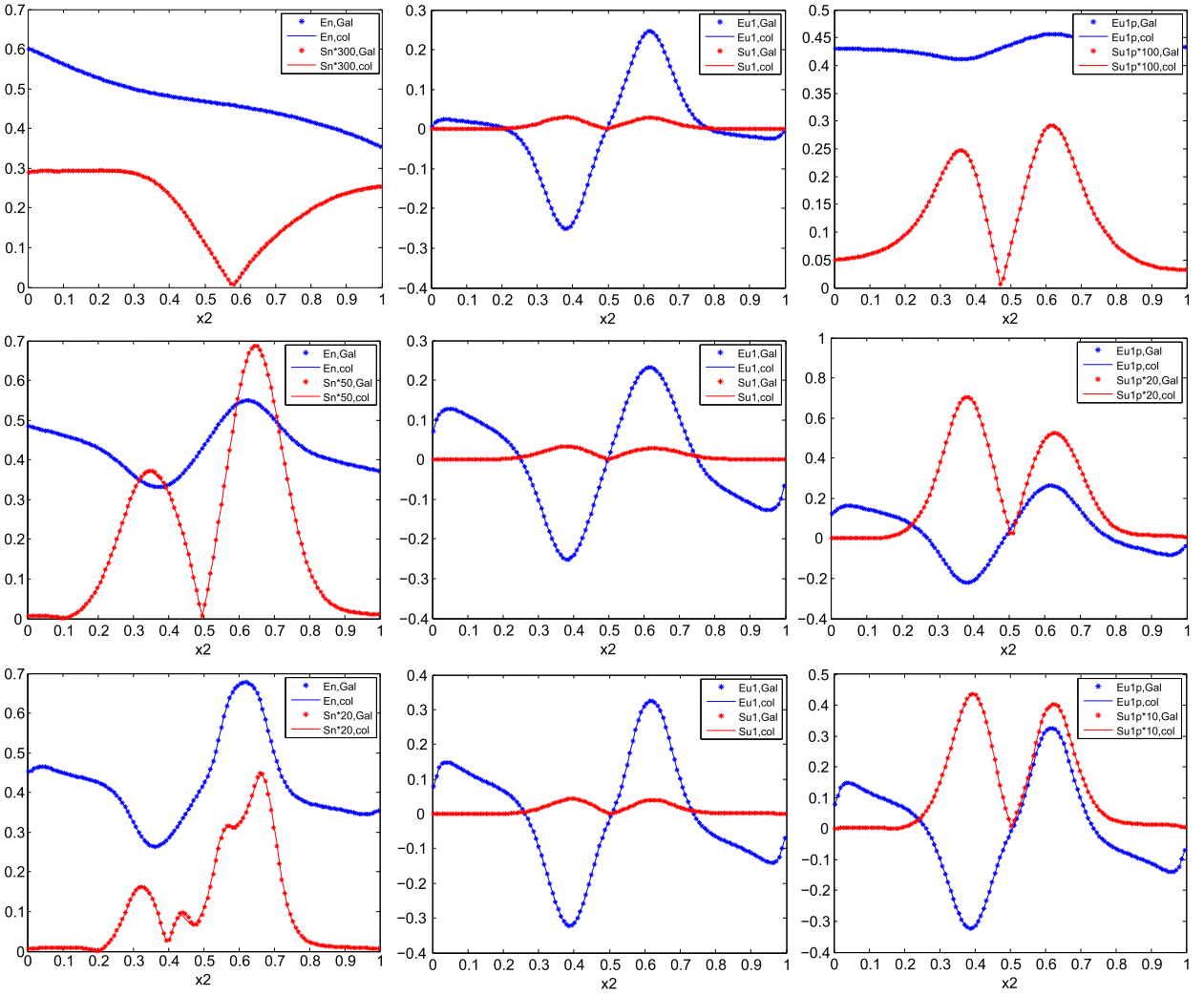


**Fig. 5.** Example 1: at $x_1 = 0.55$. Upper: $\epsilon = 1$; middle: $\epsilon = 0.01$; lower: $\epsilon = 10^{-8}$. Curve: collocation; asterisks: Galerkin. Blue: expectation; red: standard deviation. From left to right: particle density $n$, fluid velocity $u$ (first component), particle bulk velocity $\frac{J}{n}$ (first component). Some standard deviations are multiplied by constants to make them easy to observe, as noted on the figure. (For interpretation of the references to color in this figure legend, the reader is referred to the web version of this article.)

velocity, and only when $\epsilon$ is small, the interaction between the particles and the fluid is strong enough to propagate a significant amount of the initial uncertainty from the particles to the fluid.

### 5.2.3. *Example 3: random initial particle density with the normal distribution*

In this example, the random variable $\tilde{z}$ obeys the normal distribution $\mathcal{N}(0, 1)$. We take initial fluid velocity as zero and particle distribution as the equilibrium with density

$$n = 0.5 - 0.2 \arctan[10(x_1 - 0.5 + 0.1\tilde{z} + 0.2x_2)]/(\pi/2), \tag{5.8}$$

and bulk velocity as zero. This initial data is similar to Example 2, so one expects similar physical behaviors. The expectation and standard deviation of the fluid velocity and the macroscopic quantities of the particles are shown in Figs. 9, 10, 11 (for $\epsilon = 1, 0.01, 10^{-8}$ respectively). One can see that the result is similar to Example 2. One difference is that the standard deviations of Example 3 are smoother than the corresponding quantities in Example 2. This is because the Gaussian random variable $\tilde{z}$ ranges in $(-\infty, \infty)$, but the uniform random variable $z$ ranges in $[-1, 1]$. In the initial data the random variables appear as the position of the sharp gradient of $n$. Therefore with a larger range of $\tilde{z}$, the uncertainty is less concentrated in the $x$-space.

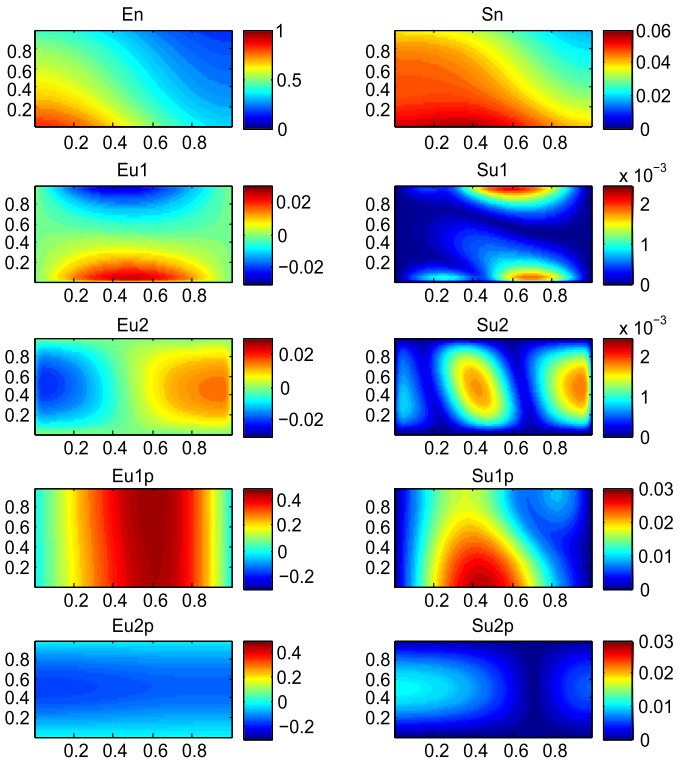


**Fig. 6.** Example 2: $\epsilon = 1$. Left column: expectation. Right column: standard deviation. Rows: particle density $n$, fluid velocity $u$ (two components), particle bulk velocity $\frac{J}{n}$ (two components).

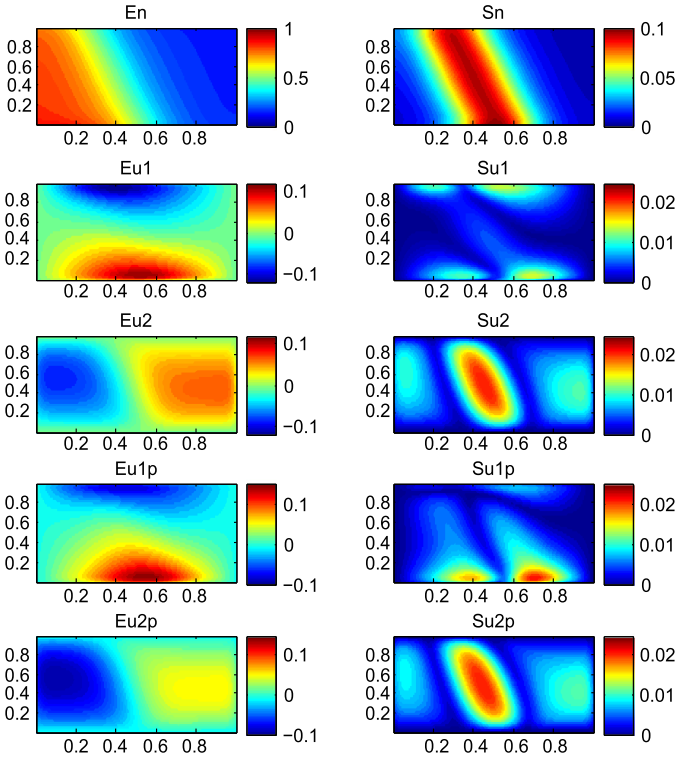


**Fig. 7.** Example 2: $\epsilon = 0.01$. Left column: expectation. Right column: standard deviation. Rows: particle density $n$, fluid velocity $u$ (two components), particle bulk velocity $\frac{J}{n}$ (two components).

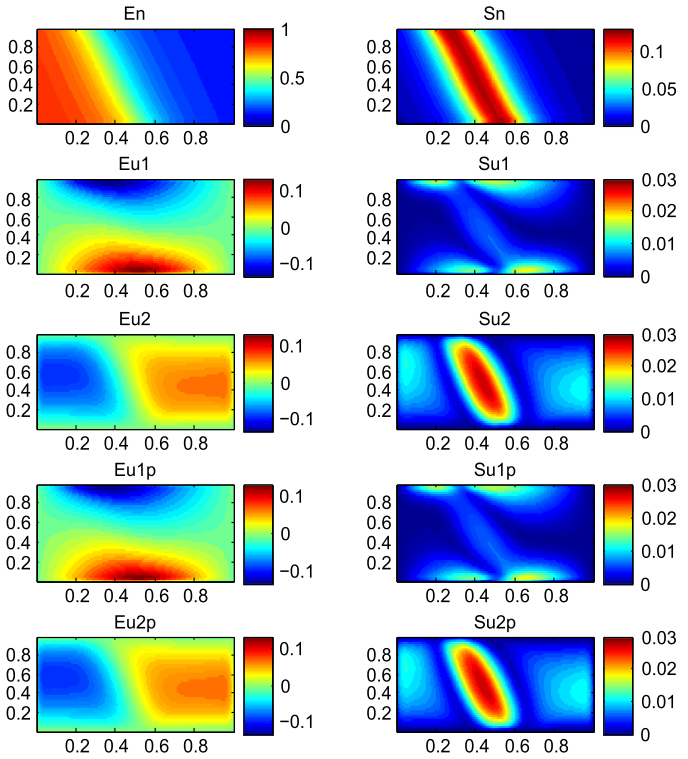


**Fig. 8.** Example 2: $\epsilon = 10^{-8}$. Left column: expectation. Right column: standard deviation. Rows: particle density $n$, fluid velocity $u$ (two components), particle bulk velocity $\frac{J}{n}$ (two components).

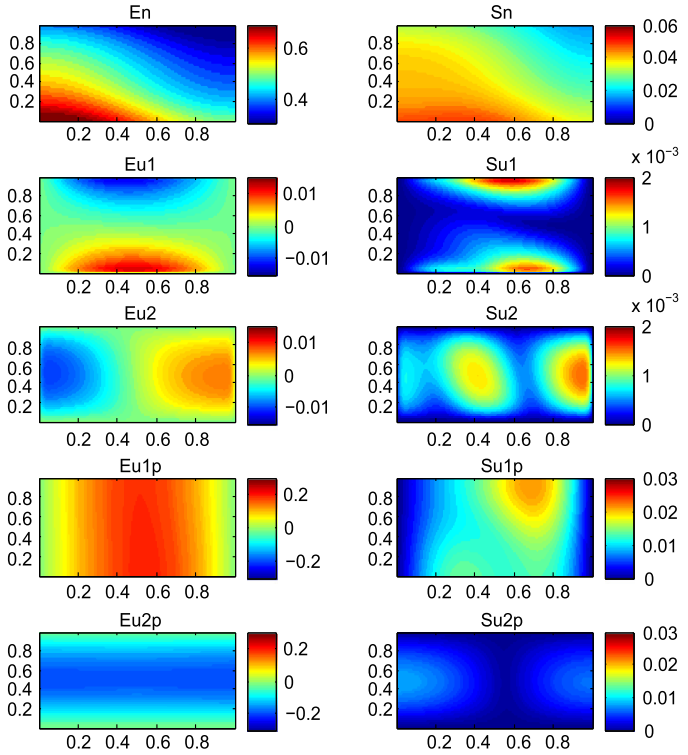


**Fig. 9.** Example 3: $\epsilon = 1$. Left column: expectation. Right column: standard deviation. Rows: particle density $n$, fluid velocity $u$ (two components), particle bulk velocity $\frac{J}{n}$ (two components).

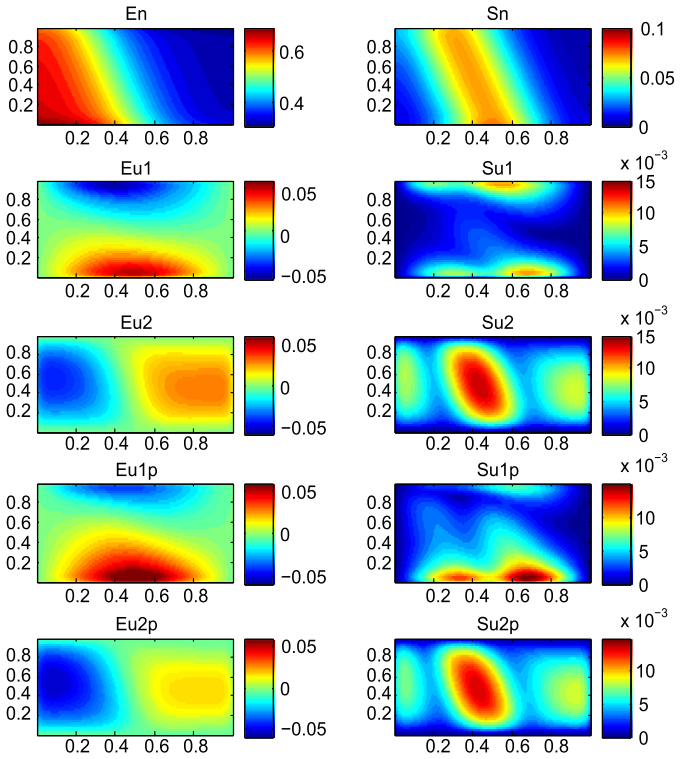


**Fig. 10.** Example 3: $\epsilon = 0.01$. Left column: expectation. Right column: standard deviation. Rows: particle density $n$, fluid velocity $u$ (two components), particle bulk velocity $\frac{J}{n}$ (two components).

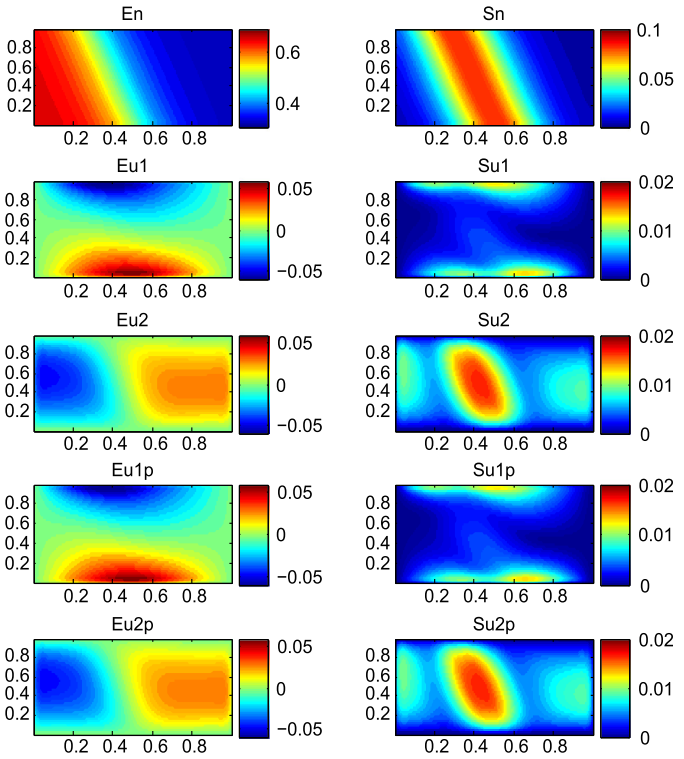


**Fig. 11.** Example 3: $\epsilon = 10^{-8}$. Left column: expectation. Right column: standard deviation. Rows: particle density $n$, fluid velocity $u$ (two components), particle bulk velocity $\frac{J}{n}$ (two components).

## 6. Conclusion

In this paper we derive a stochastic Asymptotic-Preserving (s-AP) generalized polynomial chaos expansion based stochastic Galerkin (gPC-sG) method for a kinetic-fluid model with multiscales and uncertainty, which models disperse two-phase flows. We study the structure of $\vec{\mathcal{L}}$, the gPC version of the Fokker–Planck operator, give a coercivity estimate of $\vec{\mathcal{L}}$ and determine the null space of $\vec{\mathcal{L}}$. With these properties of $\vec{\mathcal{L}}$ we derive the hydrodynamic limit of the gPC approximation of the kinetic system as the gPC approximation of the limiting Navier–Stokes system, which justifies the s-AP property. The coefficient matrices of the Helmholtz equations and the Poisson equations arising in the method are proved to be positive definite under reasonable assumptions. In the implicit treatment of $\vec{\mathcal{L}}$ one needs to compute the gPC version translation operator $\vec{\mathcal{T}}$, which will cost $N_v^2$ matrix diagonalizations of size $K+1$ if computed directly. We introduce a spectrally accurate splitting method which only requires two matrix diagonalizations, thus significantly enhanced the efficiency of the algorithm. The developed method allows us to simulate multiscale kinetic-fluid two-phase flows with uncertainty with spectral accuracy in the random space, and allows coarse meshes and large time steps even in the regime of small mean free path.

Several related problems are still open:

1. How to prove the regularity of the exact solution in the random space? This is the first step towards proving the spectral accuracy of the gPC-sG method. Papers [11,12] give estimates on the solution by using the entropy methods. However, since the $z$-derivatives of $f$ are not necessarily positive everywhere, one cannot use $\partial_z f \log(\partial_z f)$ as an entropy since $\log(\partial_z f)$ may fail to be well-defined. Therefore their methods no longer work in our case and one would prefer the $L^2$ energy estimate [33].

2. This is the beginning of the study of such problems with uncertainties. While this paper studied uncertain initial data, uncertainties may also come from boundary data, $\Phi$, $\kappa$ and $Re$. Since these quantities do not affect the equilibrium of the FP operator, one can extend our gPC-sG method to incorporate them into the method as was done in [33]. But they remain to be done for problems of application interests to see how these uncertainties will affect the dynamics and statistical moments of the physical quantities.

3. Other two-phase flow models, for example, the compressible flows [15] or the variable density incompressible flows [14], will also be studied in our future work.

## Appendix A. Inversion of the deterministic operator $\mathcal{L}_u$

Here, for readers' convenience, we give a review of the method of inversion of the deterministic operator $\mathcal{L}_u$ proposed in [19]. $\mathcal{L}_u$ can be written as

$$\mathcal{L}_u f = \sqrt{M_u}\,\tilde{\mathcal{L}}_u h, \tag{A.1}$$

where

$$h = \frac{f}{\sqrt{M_u}}, \quad \tilde{\mathcal{L}}_u h = \frac{1}{\sqrt{M_u}}\nabla_v \cdot \left( M_u \nabla_v \left( \frac{h}{\sqrt{M_u}} \right) \right), \tag{A.2}$$

and $M_u$ as defined in (2.5). The key observation is that the operator $\tilde{\mathcal{L}}_u$ is symmetric in $L_v^2$. This symmetry can be preserved by the spatial discretization

$$(\tilde{L}_u h)_{i,j} = \frac{1}{\Delta v^2}\left( h_{i,j+1} + h_{i,j-1} + h_{i+1,j} + h_{i-1,j} - \frac{\sqrt{M_{i,j+1}} + \sqrt{M_{i,j-1}} + \sqrt{M_{i+1,j}} + \sqrt{M_{i-1,j}}}{\sqrt{M_{i,j}}} h_{i,j} \right), \tag{A.3}$$

where the subindex $u$ of $M_u$ is omitted. Note that the discrete operator satisfies the well-balanced property $\tilde{L}_u(\sqrt{M_u}) = 0$. If one uses this spatial discretization to solve an equation

$$(a - \mathcal{L}_u) f = g, \tag{A.4}$$

where $a > 0$ is a constant, then the resulting system of linear equations is symmetric positive definite, and one can solve it by the Conjugate Gradient method.

## References


[1] M.J. Andrews, P.J. O'Rourke, The multiphase particle-in-cell (MP-PIC) method for dense particulate flows, Int. J. Multiph. Flow 22 (2) (1996) 379–402.

[2] I. Babuska, F. Nobile, R. Tempone, A stochastic collocation method for elliptic partial differential equations with random input data, SIAM J. Numer. Anal. 45 (3) (2007) 1005–1034.

[3] I. Babuska, R. Tempone, G.E. Zouraris, Galerkin finite element approximations of stochastic elliptic partial differential equations, SIAM J. Numer. Anal. 42 (2) (2004) 800–825.

[4] J. Back, F. Nobile, L. Tamellini, R. Tempone, Stochastic spectral Galerkin and collocation methods for PDEs with random coefficients: a numerical comparison, in: E.M. Rønquist, J.S. Hesthaven (Eds.), Spectral and High Order Methods for Partial Differential Equations, Springer-Verlag, Berlin, Heidelberg, 2011.

[5] A. Chorin, The numerical solution of the Navier–Stokes equations for an incompressible fluid, Bull. Am. Math. Soc. 73 (1967) 928–931.

[6] J. Ding, D. Gidaspow, A bubbling fluidization model using kinetic theory of granular flow, AIChE J. 36 (4) (1990) 523–538.
[7] J.K. Dukowicz, A particle-fluid numerical model for the liquid sprays, J. Comput. Phys. 35 (2) (1980) 229–253.
[8] R.G. Ghanem, P.D. Spanos, Stochastic Finite Elements: A Spectral Approach, Springer-Verlag, New York, 1991.
[9] D. Gidaspow, R. Bezburuah, J. Ding, Hydrodynamics of Circulating Fluidized Beds: Kinetic Theory Approach, Department of Chemical Engineering, Illinois Institute of Technology, Chicago, IL, USA, 1991.
[10] A.D. Gosman, E. Loannides, Aspects of computer simulation of liquid-fueled combustors, J. Energy 7 (6) (1983) 482–490.
[11] T. Goudon, P.-E. Jabin, A. Vasseur, Hydrodynamic limit for the Vlasov–Navier–Stokes equations. I. Light particles regime, Indiana Univ. Math. J. 53 (2004) 1495–1515.
[12] T. Goudon, P.-E. Jabin, A. Vasseur, Hydrodynamic limit for the Vlasov–Navier–Stokes equations. II. Fine particles regime, Indiana Univ. Math. J. 53 (2004) 1517–1536.
[13] T. Goudon, S. Jin, J.-G. Liu, B. Yan, Asymptotic-preserving schemes for kinetic-fluid modeling of disperse two-phase flows, J. Comput. Phys. 246 (2013) 145–164.
[14] T. Goudon, S. Jin, J.-G. Liu, B. Yan, Asymptotic-preserving schemes for kinetic-fluid modeling of disperse two-phase flows with variable fluid density, Int. J. Numer. Methods Fluids 75 (2014) 81–102.
[15] T. Goudon, S. Jin, B. Yan, Simulation of fluid-particles flows: heavy particles, flowing regime and asymptotic-preserving schemes, Commun. Math. Sci. 10 (2012) 355–385.
[16] Max D. Gunzburger, Clayton G. Webster, Guannan Zhang, Stochastic finite element methods for partial differential equations with random input data, Acta Numer. 23 (2014) 521–650.
[17] X. Jiang, G.A. Siamas, K. Jagus, et al., Physical modelling and advanced simulations of gas–liquid two-phase jet flows in atomization and sprays, Prog. Energy Combust. Sci. 36 (2) (2010) 131–167.
[18] S. Jin, Efficient asymptotic-preserving (AP) schemes for some multiscale kinetic equations, SIAM J. Sci. Comput. 21 (2) (1999) 441–454.
[19] S. Jin, B. Yan, A class of asymptotic-preserving schemes for the Fokker–Planck–Landau equation, J. Comput. Phys. 230 (2011) 6420–6437.
[20] Shi Jin, Asymptotic preserving (AP) schemes for multiscale kinetic and hyperbolic equations: a review, Riv. Math. Univ. Parma (N.S.) 3 (2) (2012) 177–216.
[21] Shi Jin, Dongbin Xiu, Xueyu Zhu, Asymptotic-preserving methods for hyperbolic and transport equations with random inputs and diffusive scalings, J. Comput. Phys. 289 (2015) 35–52.
[22] O.P. Le Maître, O.M. Knio, Spectral Methods for Uncertainty Quantification, Scientific Computation, with Applications to Computational Fluid Dynamics, Springer, New York, 2010.
[23] H. Niederreiter, P. Hellekalek, G. Larcher, P. Zinterhof, Monte Carlo and Quasi-Monte Carlo Methods 1996, Springer-Verlag, 1998.
[24] F. Nobile, R. Tempone, C.G. Webster, A sparse grid stochastic collocation method for partial differential equations with random input data, SIAM J. Numer. Anal. 46 (5) (2008) 2309–2345.
[25] P.J. O'Rourke, Collective Drop Effects on Vaporizing Liquid Sprays, Los Alamos National Lab., NM, USA, 1981.
[26] S.C. Saxena, Devolatilization and combustion characteristics of coal particles, Prog. Energy Combust. Sci. 16 (1) (1990) 55–94.
[27] R. Temam, Sur l'approximation de la solution des equations de Navier–Stokes par la méthode des pas fractionnarires II, Arch. Ration. Mech. Anal. 33 (1969) 377–385.
[28] D. Xiu, Fast numerical methods for stochastic computations: a review, Commun. Comput. Phys. 5 (2–4) (2009) 242–272.
[29] D. Xiu, Numerical Methods for Stochastic Computation, Princeton University Press, Princeton, New Jersey, 2010.
[30] Dongbin Xiu, Jan S. Hesthaven, High-order collocation methods for differential equations with random inputs, SIAM J. Sci. Comput. 27 (3) (2005) 1118–1139 (electronic).
[31] Dongbin Xiu, George Em Karniadakis, The Wiener–Askey polynomial chaos for stochastic differential equations, SIAM J. Sci. Comput. 24 (2) (2002) 619–644 (electronic).
[32] X. Zhang, C.-W. Shu, On positivity-preserving high order discontinuous Galerkin schemes for compressible Euler equations on rectangular meshes, J. Comput. Phys. 229 (23) (2010) 8918–8934.
[33] Y. Zhu, S. Jin, The Vlasov–Poisson–Fokker–Planck system with uncertainty and a one-dimensional asymptotic-preserving method, Preprint, 2016.